10th Oxford School on Neutron Scattering

4-14 September 2007

University of Oxford, Mansfield College

EXERCISE BOOK

CONTENTS

Supported by:

ISIS NEUTRONS FOR SCIENCE nmi3

http://www.oxfordneutronschool.org/

A. Single-Crystal Diffraction

Exercises A

Answer the following questions:

A1.

2.20 km/sec is conventionally taken as a standard velocity for thermal neutrons. (For example, absorption cross sections are tabulated for this value of the velocity.)

(i) Using the de Broglie relation show that the wavelength of neutrons with this standard velocity is approximately 1.8*Å*.

(ii) What is the kinetic energy of these neutrons? (See values of physical constants, p22.)

(iii) What is the energy of an X-ray photon of wavelength $\lambda = 1.8Å$?

(iv) Calculate the velocity of a neutron which has the same energy as this X-ray photon.

A2.

A beam of 'white' neutrons emerges from a collimator with a divergence of $\pm 0.2^{\circ}$. It is then Bragg reflected by the (111) planes of a monochromator consisting of a single-crystal of lead.

(i) Calculate the angle between the direct beam and the [111] axis of the crystal to produce a beam of wavelength $\lambda = 1.8Å$. (Unit cell edge $\mathbf{a}_0$ of cubic lead is 4.94*Å*.)

(ii) What is the spread in wavelengths of the reflected beam?

*Questions **A3** and **A4** are concerned with the treatment of Bragg scattering in reciprocal space. **A3** refers to the scattering of neutrons of a fixed-wavelength, and **A4** to the scattering of pulsed neutrons covering a wide band of wavelengths.*

A3.

A single crystal has an orthorhombic unit cell with dimensions $a = 6\text{Å},\ b = 8\text{Å},\ c = 10\text{Å}$. Plot the reciprocal lattice in the $\mathbf{a}^*\mathbf{b}^*$ plane adopting a scale of $1\text{Å}^{-1} = 20mm$.

A horizontal beam of neutrons of wavelength $\lambda = 1.8\text{Å}$ strikes the crystal. The crystal is rotated about its vertical **c** axis between the settings for the *630* and *360* reflections.

Draw the Ewald circles for these two reflections. How many *hk0* reflections will give rise to Bragg scattering while the crystal is rotated beween *630* and *360* ?

A4.

Pulsed neutrons with a wavelength range from 1.5Å to 5.0Å undergo Bragg scattering from this crystal. The horizontal neutron beam is parallel to the **a** axis of the crystal and strikes the crystal at right angles to the **c** axis. Using the Ewald construction find the maximum number of Bragg reflections which can be observed simultaneously in the horizontal scattering plane.

A5.

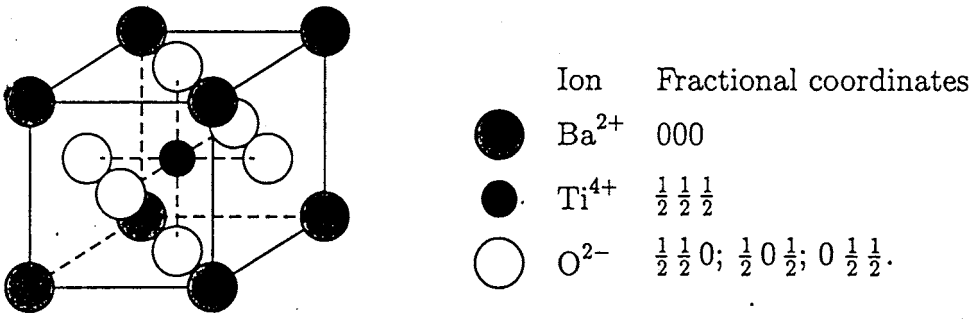

The diagram shows the high-temperature cubic unit cell of $BaTiO_3$ alongside a list of the fractional coordinates of the ions in the unit cell. Show that the intensity $I_{(00l)}$ of the neutron beam diffracted from the (00*l*) planes of cubic $BaTiO_3$ is proportional to

$$[b_{Ba} + (-1)^l b_{Ti} + \{1 + 2\ \mathbf{x}\ (-1)^l b_O\}]^2,$$

where b_{Ba}, b_{Ti} and b_O are the coherent scattering lengths of the nuclei.

On cooling through the ferroelectric transition temperature $T_c = 130^{\circ}C$ the structure of $BaTiO_3$ undergoes a displacive transition in which the Ti^{4+} and O^{2-} ions move in opposite directions relative to the Ba^{2+} ions. As a first approximation the fractional coordinates of the ions in the distorted phase are

Ba^{2+}	0,0,0
Ti^{4+}	½,½,½+δ
O^{2-}	½,½,-δ; ½,0, ½-δ; 0, ½, ½-δ;

where $\delta \ll 1$.

The intensity of the (005) neutron diffraction peak from a single crystal of $BaTiO_3$ is found to increase by 74% on cooling the crystal through T_c. Use this observation to determine δ.

Explain why it is advantageous to use neutron diffraction, rather than X-ray diffraction, to determine the ionic displacements.

[Coherent scattering lengths: $b_{Ba} = 5.25 \times 10^{-15}$ m, $b_{Ti} = -3.30 \times 10^{-15}$ m, $b_O = 5.81 \times 10^{-15}$ m; atomic numbers: $Z_{Ba} = 56$, $Z_{Ti} = 22$, $Z_O = 8$.]

Oxford Physics Hons '03

B. Coherence and Incoherence

Exercises B

Atoms with just one isotope and with zero nuclear spin have a neutron scattering amplitude b, which may be considered to be the counterpart of the 'X-ray atomic scattering factor' f. The amplitude b is the same for each atom in the sample which belong to the same element in the Periodic Table, and scattering formulae tend to be the same as for X-rays with b exchanged for f. However, the situation is more complicated if the nucleus has non-zero spin, or if the atom is present as a mixture of different isotopes, or if both situations occur.

Neutron scattering lengths (amplitudes) vary between different isotopes of the same element, and (if the nucleus has a non-zero spin) between the different spin states of the same nucleus. Hence a neutron beam striking a sample is scattered by an array of nuclei possessing a random distribution of different scattering lengths. The scattering is divided into a "coherent" part whose magnitude is determined by the average scattering length throughout the sample, and an "incoherent" part determined by the spread of the scattering lengths about this average. The coherent scattering gives information on the correlation between the positions of ***different*** *nuclei at different times, whereas the incoherent scattering depends only on the correlation between the positions of the* ***same*** *nucleus at different times.*

A neutron of spin $\frac{1}{2}$ *interacts with a nucleus of spin I to form two states in which the combined spins are parallel or antiparallel. The spin J of these states is then* $J = I + \frac{1}{2}$ *and* $J = I - \frac{1}{2}$*, respectively. Different scattering lengths* b^+, b^- *are associated with these states. The fractional occupancies* w^+, w^- *of the states are determined by the number of spin orientations of each state. This number is* $2J+1$*, and so* $w^+ = (I+1)/(2I+1)$ *and* $w^- = I/(2I+1)$.

Let us suppose that the atom contains several isotopes and that the scattering lengths of the r^{th} *isotope, with fractional occupancies* w_r^+ *and* w_r^-*, are* b_r^+ *and* b_r^-. *The coherent scattering length* b^{coh} *of the atom is the scattering length averaged over all the isotopes and the spin states, i.e.*

$$b^{coh} = \sum_r c_r \left(w_r^+ b_r^+ + w_r^- b_r^- \right), \qquad \text{(B1)}$$

where c_r *is the abundance of the rth isotope. The coherent scattering cross section is given by:*

$$\sigma_{coh} = 4\pi\left(b^{coh}\right)^2. \qquad \text{(B2)}$$

The total cross section is obtained by adding the separate contributions of the individual isotopes r and spin states $\pm$:

$$\sigma_{tot} = 4\pi\sum_r c_r\left[w_r^+\left(b_r^+\right)^2 + w_r^-\left(b_r^-\right)^2\right]. \qquad \text{(B3)}$$

Finally, the incoherent scattering cross section σ_{incoh} is the difference between the total and coherent cross sections:

$$\sigma_{incoh} = \sigma_{tot} - \sigma_{coh}$$

i.e.

$$\sigma_{incoh} = 4\pi\sum_r c_r\left[w_r^+\left(b_r^+\right)^2 + w_r^-\left(b_r^-\right)^2\right] - 4\pi\left(\sum_r c_r\left(w_r^+ b_r^+ + w_r^- b_r^-\right)\right)^2. \qquad \text{(B4)}$$

Answer the following questions:

B1

Table B.1 gives the spin I of the nuclei of hydrogen and deuterium, together with the measured values of the scattering lengths of the systems with combined spins $I+\frac{1}{2}$ and $I-\frac{1}{2}$. Calculate the values of σ_{coh} and σ_{incoh} for H^1 and H^2.

Table B.1.

	spin I	b^+ (x10^{-14}m)	b^- (x10^{-14}m)
hydrogen	1/2	1.085	-4.75
deuterium	1	0.953	0.098

You will find that , whereas σ_{incoh} for deuterium is much smaller than σ_{coh} , the reverse is true for the scattering of neutrons by hydrogen. This means

that hydrogen/deuterium labelling is of great importance in both diffraction and spectroscopic studies.

B2

Table B.2 gives the experimental values of the scattering lengths and the abundance of the individual isotopes of nickel: ^{58}Ni, ^{60}Ni, ^{61}Ni, ^{62}Ni and ^{64}Ni. With the exception of ^{61}Ni, the isotopes have zero spin and so b^+ is the same as b^-. Calculate the values of σ_{coh} and σ_{incoh} for natural nickel containing all five isotopes.

Table B.2.

isotope r	**abundance** c_r	**spin** I	b_r^+ $(10^{-14}\,\mathrm{m})$	b_r^- $(10^{-14}\,\mathrm{m})$
58	68.3%	0	1.44	1.44
60	26.1%	0	0.28	0.28
61	1.1%	3/2	0.46	1.26
62	3.6%	0	-0.87	-0.87
64	0.9%	0	-0.04	-0.04

C. Time-of-Flight Powder Diffraction

Exercises C

Answer the following questions:

C1.

(a) In a time-of-flight powder diffraction experiment the incident beam is pulsed , and with each pulse a polychromatic burst of neutrons strikes the sample. The different wavelengths λ in a pulse are separated by measuring their time-of-flight t from source to detector. Using the table of physical constants show that the relation between wavelength and t.o.f. is given by

$$t(\text{in } \mu secs) = 252.8\lambda\,(\text{in } \mathring{A}) \text{ x } L(\text{in metres})$$

where L is the total flight path.

(b) A powder diffractometer, with $L = 100\,m$ and scattering angle $2\theta = 170^\circ$, was used to obtain the t.o.f. diffraction pattern of perovskite, $CaTiO_3$. Calculate the values of t for the three Bragg reflections with the longest times of flight. ($CaTiO_3$ crystallises in a primitive cubic lattice with a unit cell of edge a_0 = 3.84Å.)

(c) For a sample with a cubic unit cell, show that the time-of-flight t of each Bragg peak in the t.o.f. powder diffraction pattern is related to its indices hkl by:

$$t \propto \left(h^2 + k^2 + l^2\right)^{-1/2} . \qquad \text{(C1)}$$

C2.

Silicon crystallises in the face-centred-cubic structure of diamond with the lattice points at:

$$000;\ \tfrac{1}{2}\tfrac{1}{2}0;\ \ \tfrac{1}{2}0\tfrac{1}{2};\ 0\tfrac{1}{2}\tfrac{1}{2}.$$

In this structure there is a primitive basis of two identical atoms at 000 *and* $\tfrac{1}{4}\tfrac{1}{4}\tfrac{1}{4}$ *which is associated with each lattice point of the unit cell.*

(a) Show that the indices *hkl* of the Bragg reflections for the face-centred cubic (f.c.c.) lattice are all odd or all even.

(b) Show that reflections with an odd value of $(h+k+l)/2$, such as *222* and *442*, are forbidden.

(c) From eqn. (C1) the Bragg reflections in the t.o.f. powder pattern are separated according to their values of $\left(h^2+k^2+l^2\right)$. In Table C.1 all the possible values of $\left(h^2+k^2+l^2\right)$ are listed in the order of decreasing time-of-flight for the range

$$1<\left(h^2+k^2+l^2\right)<52.$$

(This is the range covered in Figure C.1 below.)

Table C.1. Sums of three squared integers.

$h^2+k^2+l^2$	$h^2+k^2+l^2$	$h^2+k^2+l^2$	$h^2+k^2+l^2$	$h^2+k^2+l^2$
1	11*	21	33	43*
2	12*	22	34	44*
3*	13	24*	35*	45
4*	14	25	36*	46
5	16*	26	37	48*
6	17	27*	38	49
8*	18	29	40*	50
9	19*	30	41	51*
10	20*	32*	42	52*

The values of $h^2+k^2+l^2$ in which the integers are all odd or all even are marked with asterisks.

(i) What are the indices *hkl* corresponding to these asterisks?

(ii) Which of the f.c.c. reflections are forbidden?

(iii) Which of the allowed f.c.c. reflections overlap with one another?

(d) Figure C.1 shows the diffraction pattern of powdered silicon, taken with a time-of-flight diffractometer installed at the pulsed neutron source of the electron

linear accelerator at the Harwell Laboratory. The scattering angle was $2\theta = 167^\circ$ and the path length $L = 14m$. *To avoid frame overlap the Bragg peak with the longest flight time was cut out of the spectrum.*

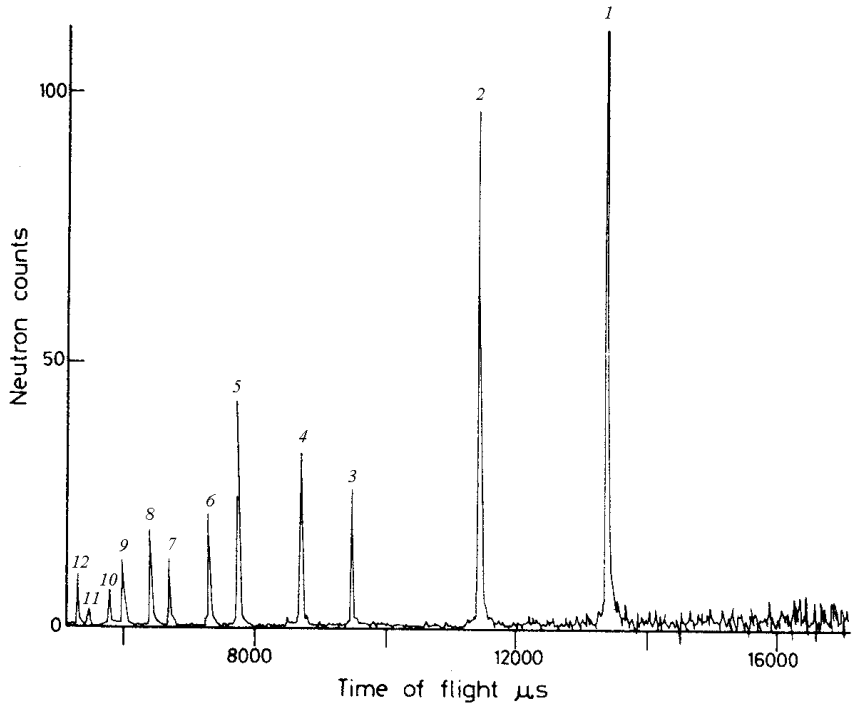

Figure C.1. Time-of-flight diffraction pattern of powdered silicon. The observed spectrum has been ratioed with a vanadium spectrum: vanadium is an incoherent scatterer whose spectrum gives the wavelength dependence of the incident neutron flux.
(*After* Willis, 1983.)

The values of t for the twelve numbered Bragg peaks in Figure C.1 were measured (to a precision of less than $1\mu sec$) giving the results in Table C.2.

Index all these peaks and determine the linear size a_0 of the unit cell of silicon.

Table C.2

peak number	time of flight $(\mu sec\, s)$
1	13 503
2	11 515
3	9 549
4	8 760
5	7 796
6	7 351
7	6 753
8	6 455
9	6 038
10	5 823
11	5 513
12	5 348

C3.

In a time-of-flight neutron powder diffractometer, a sharp pulse of neutrons with a range of wavelengths is fired at the sample. The diffracted signal is measured at a fixed scattering angle 2θ, and the diffraction pattern comes from measurements of the time taken for the neutrons in a single pulse to travel the distance *l* from the source to the detector. Using the de Brogue relationship, together with the Bragg relationship, show that the time *t* taken by the neutrons to travel the distance *l* is related to the size of the d-spacing

$$d = \frac{ht}{2ml\sin\theta}$$

of a given reflection by

where *m* is the mass of the neutron.

No quantities are known exactly. For an uncertainty of Δθ on the Bragg

$$\Delta d = \frac{\partial d}{\partial \theta}\Delta\theta$$

angle, error analysis gives the corresponding uncertainty on *d:*

Show by differentiation of the Bragg law that for a given uncertainty Δθ this

$$\left|\frac{\Delta d}{d}\right| = \cot\theta\Delta\theta$$

leads to a maximum resolution of

In order to optimize the resolution of a time-of-flight powder diffractometer, the scattering angle 2θ is chosen to be as close to 180° as possible. In this case a significant source of uncertainty is in the distance travelled by the neutron beam. Show that the uncertainty in the flight path l of Δl leads to a resolution limit of

$$\frac{\Delta d}{d} = \frac{\Delta l}{l}$$

If the uncertainty in the value of l comes from the width of the neutron moderator of 2 cm, calculate the flight paths necessary to achieve (a) a moderate resolution of $\Delta d/d = 10^{-3}$, and (b) a high resolution $\Delta d/d = 2 \times 10^{-4}$. Comment on your answers, and check out the real situation at the ISIS spallation neutron source by looking at the instruments POLARIS and HRPD from http://www.isis.rl .ac.uk.

M. Dove '03

D. Magnetic Elastic Scattering

Exercises D

Introduction

In general, the scattering of neutrons by atoms is a nuclear process. However, in the case of magnetic atoms with unpaired electrons there is an additional scattering which arises from the interaction between the magnetic moment of the neutron and the magnetic moment of the atom.

The magnetic interaction gives rise to an atomic scattering amplitude p, which is given in the dipole approximation by

$$p = \left(\frac{e^2 \gamma}{m_e c^2} \right) Sf \quad . \tag{D1}$$

(p is the magnetic counterpart of the nuclear scattering amplitude b .) The factor $\frac{e^2}{m_e c^2}$ *in eqn (D1) is the classical radius of the electron , S is the spin quantum number of the atom , γ is the magnetic moment of the neutron expressed in nuclear magnetons , and f is a magnetic form factor. (We assume that the magnetism arising from the angular momentum of the unpaired electron is 'quenched': this is a good assumption for salts of the transition elements.) Substituting the numerical values of the constants into eqn (D1) gives*

$$p = 0.54 Sf \times 10^{-14} m \quad .$$

The magnitude of p is on the same scale as that of the nuclear scattering amplitude b. Hence, in an ordered magnetic material, such as ferromagnetic Fe or antiferromagnetic MnO, the intensity of Bragg magnetic scattering is comparable to the intensity of Bragg nuclear scattering.

The magnetic structures of many materials have been determined by magnetic neutron diffraction. The exercises below illustrate some of the features associated with this kind of study.

Answer the following questions:

(Questions **D1** and **D2** relate to the system MnO. For those who are familiar with magnetic scattering, ignore **D1** and **D2** and go on to **D3.** Question **D3** relates to the system MnF_2 and is more difficult!)

D1

Manganese oxide, MnO, has the cubic-rocksalt crystal structure ($a_0 \approx 4.43$Å) with atoms at the following positions in the chemical unit cell:

$$Mn: \ 000, \ \tfrac{1}{2}\tfrac{1}{2}0, \ \tfrac{1}{2}0\tfrac{1}{2}, \ 0\tfrac{1}{2}\tfrac{1}{2}$$

$$O: \ \tfrac{1}{2}00, \ 0\tfrac{1}{2}0, \ 00\tfrac{1}{2}, \ \tfrac{1}{2}\tfrac{1}{2}\tfrac{1}{2} \ .$$

At low temperatures it is antiferromagnetic. As it is cooled below the Néel temperature, magnetic reflections appear at $\left\{\frac{h}{2} \ \frac{k}{2} \ \frac{l}{2}\right\}$ *where the Miller indices* h, k, l *are all odd. This observation shows that the magnetic unit cell is twice the chemical unit cell along all three cubic edges, and that the spins on the Mn ions are aligned antiferromagnetically along the* $\langle 100 \rangle$ *directions (see Figure D.1). Note that the spins order ferromagnetically on one set of* $\{111\}$ *planes with antiferromagnetic coupling between neighbouring* $\{111\}$ *planes.*

Show that the Bragg peaks of antiferromagnetic MnO are entirely of nuclear origin or entirely of magnetic origin but are not a mixture of both.

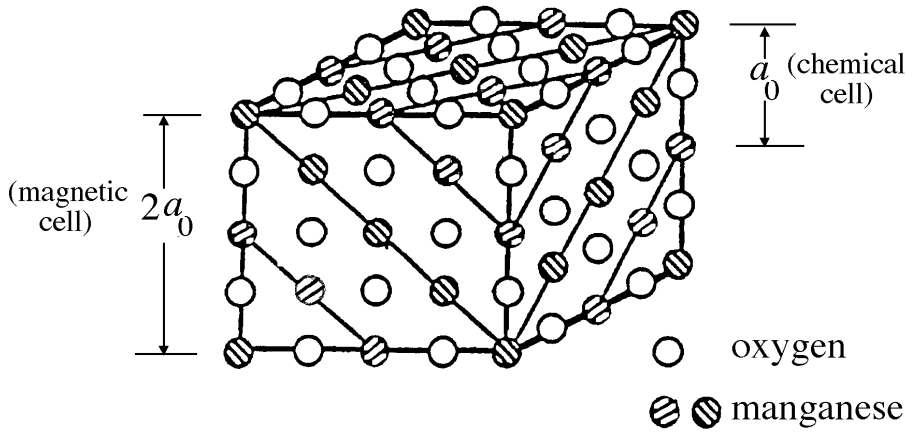

Figure D.1. Magnetic unit cell of MnO. The spins of the manganese ions lying along the $\langle 100 \rangle$ directions are alternately parallel and antiparallel.

D2

If the crystal exists as a single magnetic domain, the intensity of a magnetic Bragg peak from a single crystal of MnO is proportional to $\sin^2 \alpha$, where α is the angle between the spin direction of Mn and the scattering vector. What is the value of α for the *111* and *311* reflections, when the spin direction is along:
(a) [*100*], (b) [*111*]?

Which is the more likely spin direction of the Mn ions: (a) or (b)?

D3.

MnF_2 crystallises in the rutile structure of TiO_2, illustrated in Figure D2. The unit cell is tetragonal with a = 4.8736Å and c= 3.3101Å and the atomic coordinates are:

Mn in 2(a) at 0,0,0 and 1/2,1/2,l/2
F in 4(f) at ± u,u,0; u+1/2, 1/2-u,1/2 with u=0.305.

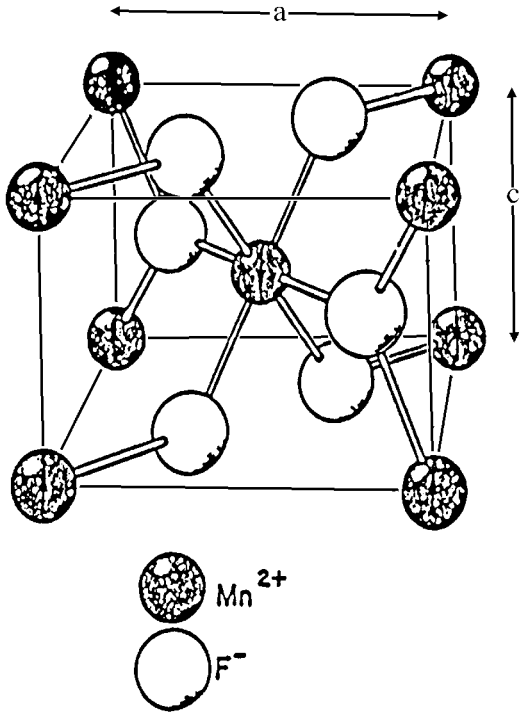

Figure D2. Chemical unit cell of manganese fluoride.]

Long range magnetic ordering takes place below the Néel temperature of 80 K. The lines with the longest d-spacings in a neutron powder pattern taken at room temperature have d-spacings of 3.446, 2.738, 2.437, 2.388 and 2.180Å. On cooling the sample below 80 K, additional magnetic lines with d-spacings 4.873, 2.388 and 2.180 Å appear in the pattern. (The last two are superimposed on lines of the same spacings arising from chemical ordering.) Figure D3 shows the powder pattern recorded by Erickson [Phys. Rev. **90**, p. 779 (1953)].

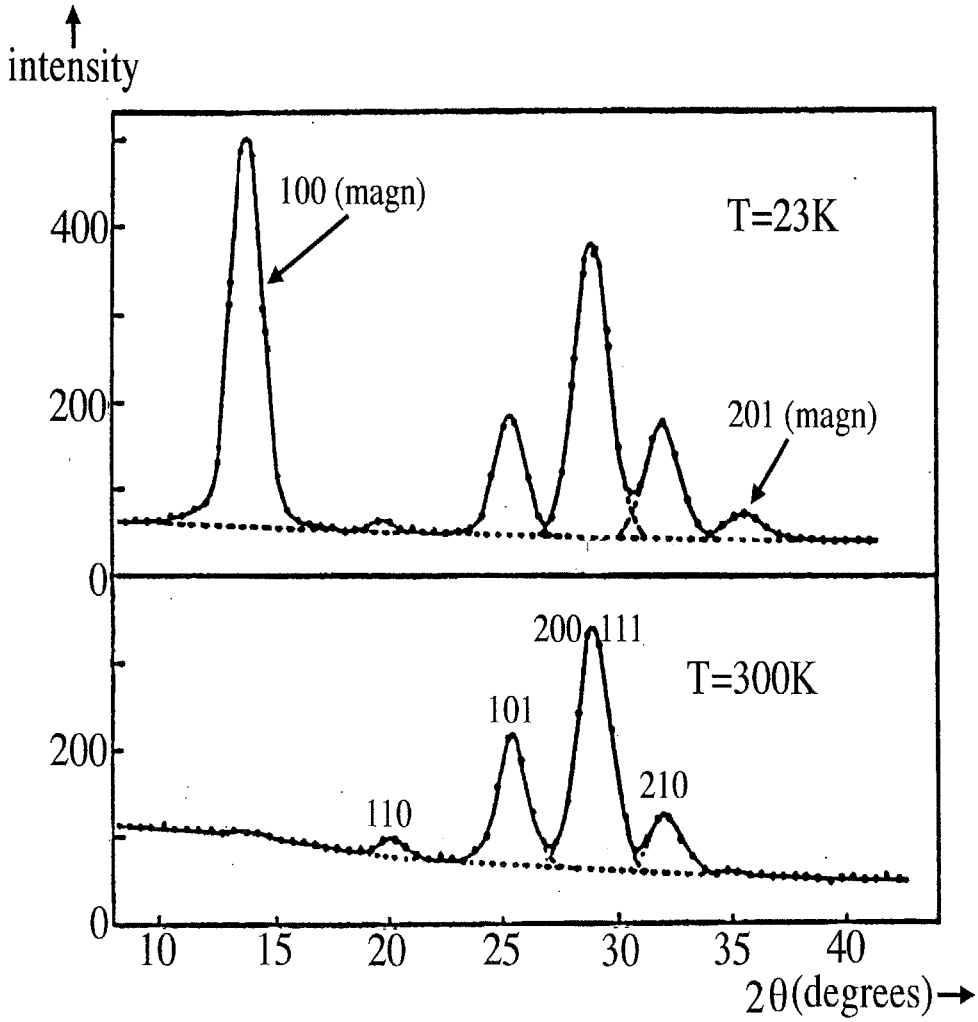

Figure D3. Neutron powder patterns of MnF_2 in the antiferromagnetic (23K) and paramagnetic (300K) states. (*After* Erickson, 1953.)

Index the lines in the ambient temperature pattern.

Does the magnetic scattering occur at positions which can be indexed on the chemical unit cell?

Is the structure commensurate or incommensurate?

What is the magnetic configuration?

What is the direction of the magnetic moments on the Mn^{2+} ions?

E. Incoherent Inelastic Scattering (with a Pulsed Neutron Spectrometer)

Exercises E

IRIS is an "inverted-geometry" spectrometer, which is installed at the pulsed neutron source ISIS. A white beam of neutrons strikes the sample, and is scattered to the pyrolytic-graphite analyser. The 002 planes of the analyser Bragg reflect the neutrons to the detector. The distance from the moderator to the sample is 36.54 m, and the distance sample-to-analyser-to-detector is 1.47 m. (See Figure E1.)

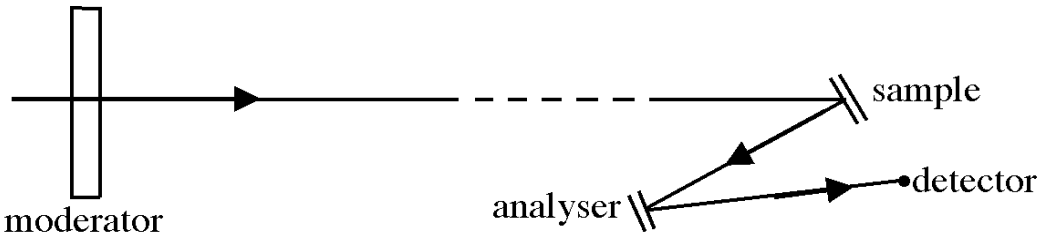

Figure E.1. Geometry of IRIS spectrometer.

The IRIS spectrum shown in Figure E 2 is for a sample of ammonia intercalated between the layers of oriented graphite. The central peak corresponds to elastic scattering by the sample , and the two outer peaks arise from inelastic scattering due to the tunnelling of hydrogen atoms between adjacent potential wells of the ammonia molecule.

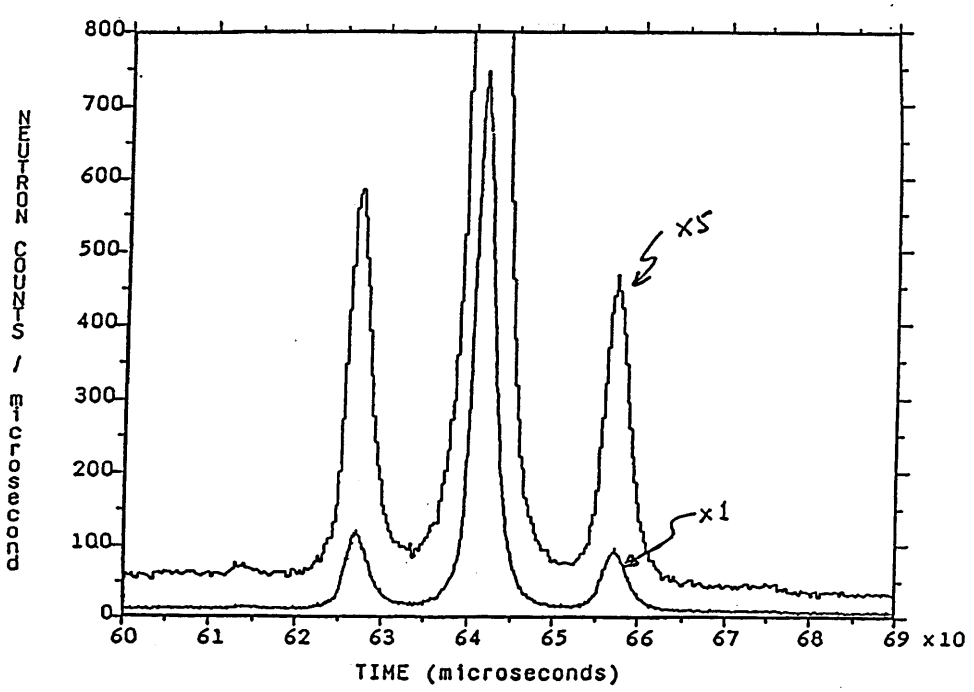

Figure E.2. IRIS spectrum of ammonia intercalated in graphite.

Answer the following questions:

E1.

(i) What is the energy selected by the crystal analyser ?

(ii) The *c*-spacing of pyrolytic graphite is 6.70Å. What is the Bragg angle θ_A of the analyser?

(iii) What is the advantage of using such a high take-off angle ($2\theta_A$) for the analyser?

E2.

Identify the peaks in the spectrum which are associated with energy gain and with energy loss. What is the magnitude of the energy transfer for these peaks ?

E3.

(i) Why are the intensities of the energy-gain and energy-loss peaks different ?

(ii) What does this difference tell us about the temperature of the sample ?

F. Coherent Inelastic Scattering (with a Triple-Axis Spectrometer)

Exercises F

Introduction

One of the most important instruments used in neutron scattering is the triple-axis spectrometer. A schematic drawing of the machine is shown in Figure F1. By employing a monochromatic neutron beam of a definite wave-vector $\mathbf{k}_i$ *(of magnitude* $k_i = 2\pi / \lambda_i$ *with* λ_i *the incident wavelength) , which is incident on a single crystal in a known orientation, and by measuring the final wave-vector* $\mathbf{k}_f$ *after scattering by the sample, we can examine excitations such as phonons (in which the atoms are excited by thermal vibrations) or magnons (in which the spin system of the atom is excited).*

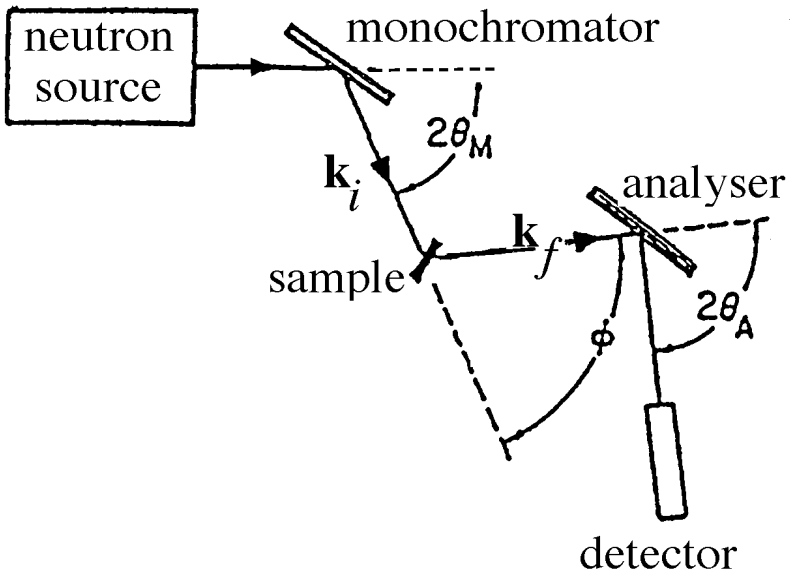

Figure F.1. Triple-axis spectrometer.

The triple-axis instrument appears to be complicated, but it is conceptually simple and every movement may be mapped by considering the so-called scattering triangle (Figure F.2). In practice, what is difficult about a triple-axis machine is that there are many different ways of performing an experiment, and choosing the appropriate configuration is often the key to performing a successful experiment. This is in contrast to a powder diffraction experiment, where one simply puts the sample in the beam and records the diffraction pattern. (See Section C).

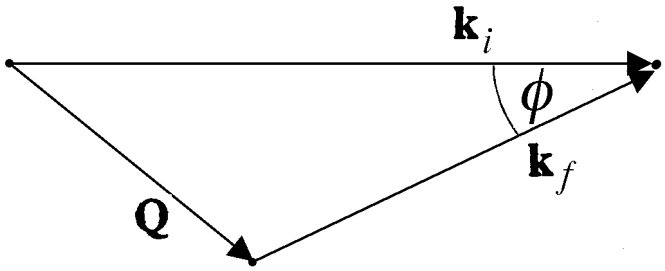

Figure F.2. Scattering triangle representing the momentum $\hbar\mathbf{Q}$ transferred to the sample when the wave vector of the neutron changes from $\mathbf{k}_i$ to $\mathbf{k}_f$. ϕ is the scattering angle.

In the following we shall consider how one actually measures a phonon excitation, using various diagrams in reciprocal space to represent the process. We use formulae which apply to all scattering processes (both neutrons and X-rays).

Momentum conservation gives

$$\mathbf{Q} = \mathbf{k}_i - \mathbf{k}_f \tag{F1}$$

where $\mathbf{Q}$ *is the scattering vector. If* ϕ *is the angle between* $\mathbf{k}_i$ *and* $\mathbf{k}_f$*, we have*

$$Q^2 = k_i^2 + k_f^2 - 2k_i k_f \cos\phi . \tag{F2}$$

Energy conservation gives

$$\Delta E = E_i - E_f , \tag{F3}$$

where E_i *is the energy of the incident neutron,* E_f *is its energy after scattering, and* ΔE *is the energy transferred to the scattering system.* ΔE *may be positive (neutrons lose energy) or negative (neutrons gain energy). If* k $(= 2\pi / \lambda)$ *is the wave-number of a neutron, its energy* E *is related to* k *by*

$$E = \frac{81.8}{\lambda^2} = 2.072k^2 \tag{F4}$$

where E *is in meV,* λ *is in Å and* k *is in Å^{-1} .*

For the following exercises, which were devised by Prof. G. H. Lander, you must imagine that you wish to investigate the low-energy spectra of silver chloride, AgCl, which is a cubic crystal with a face-centred cubic unit cell. You have been allocated time on a triple-axis spectrometer, which works with incident neutrons of energy from 3 to 14 meV.

Figure F.3 shows the (110) plane of reciprocal space . The cubic lattice parameter a_0 of AgCl is 5.56Å. One reciprocal lattice unit (rlu) is equal to $2\pi/a_0$ or 1.13Å^{-1}. The vector from the origin to any point hkl of the reciprocal lattice is of length $2\pi/d_{hkl}$, where d_{hkl} is the spacing of the hkl planes in the direct lattice.

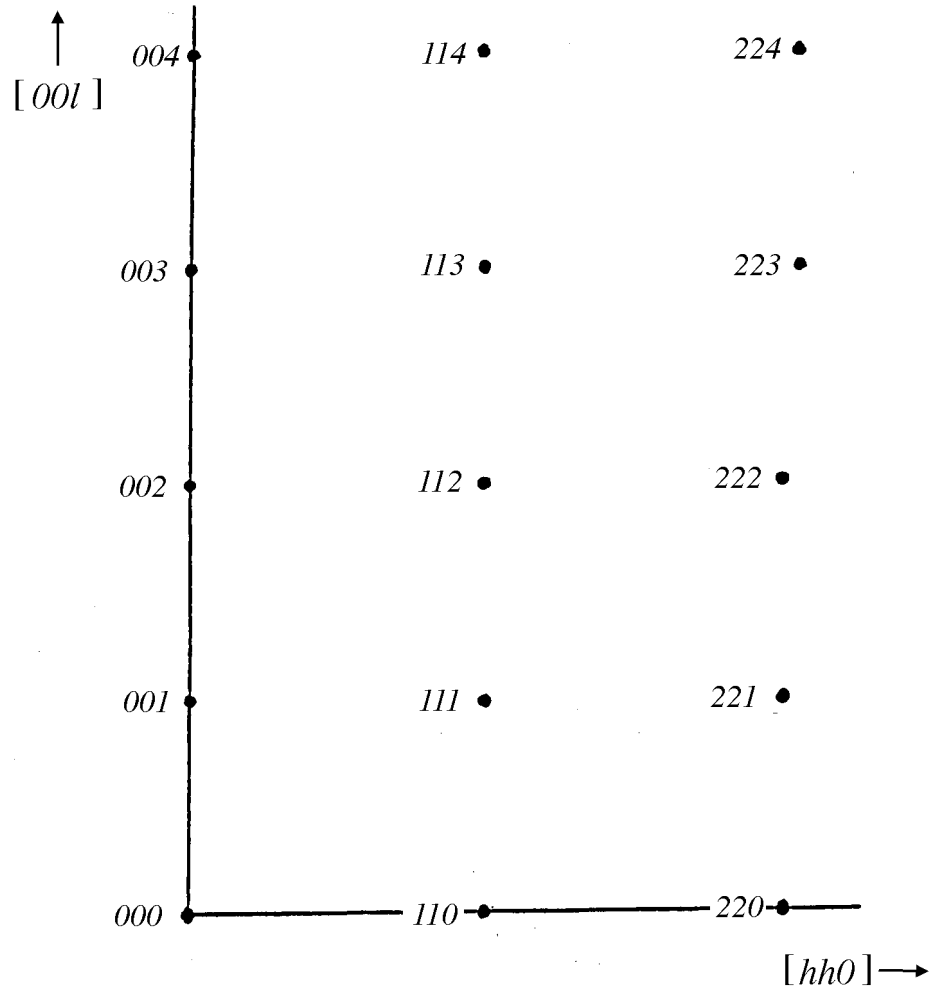

Figure F.3. (110) plane in reciprocal space of cubic crystal.

Answer the following questions:

F1

Which are the allowed points (giving non-zero Bragg reflections) of the reciprocal lattice in Figure F.3 ? Mark them with a closed circle—they are the so-called zone-centres of the Brillouin zone. Mark the disallowed points with open points—these are the zone-boundaries of the Brillouin zone. (Note that the reciprocal lattice of a face-centred cubic crystal is a body-centred cubic lattice.)

F2

E_i ranges from 3 to 14*meV*. Calculate the maximum and minimum values of the wavelength λ_i and the wave number k_i of the incident beam.

F3.

We shall begin our experiment using the maximum value of k_i *and orienting our crystal to find the 220 Bragg reflection. The scattering we observe is elastic scattering, which is much stronger than the inelastic scattering.*

(i) What is the magnitude of $\mathbf{Q}_{220}$ $(= 2\pi/d_{220})$?

Draw $\mathbf{Q}$, $\mathbf{k}_i$ and $\mathbf{k}_f$ for the *220* reflection.

(ii) What is the angle ϕ between $\mathbf{k}_i$ and $\mathbf{k}_f$?

(iii) What is the relation between the Bragg angle θ_B at the sample and ϕ ?

F4.

We can now start our inelastic experiment. Consider the dispersion curves for AgCl shown in Figure F.4 Let us suppose that we wish to measure the phonon with a reduced wave vector of 0.4 propagating in the [001] direction and and that the phonon is transverse acoustic. (A shorthand notation for this is TA[001].) Using the conversion tables on p.2 we see that the energy of this phonon is about 3meV.

In Figure F3 draw the wave-vector $\mathbf{q}$ of this phonon away from the *220* zone-centre. (By zone-centre we mean $q = 0$.)

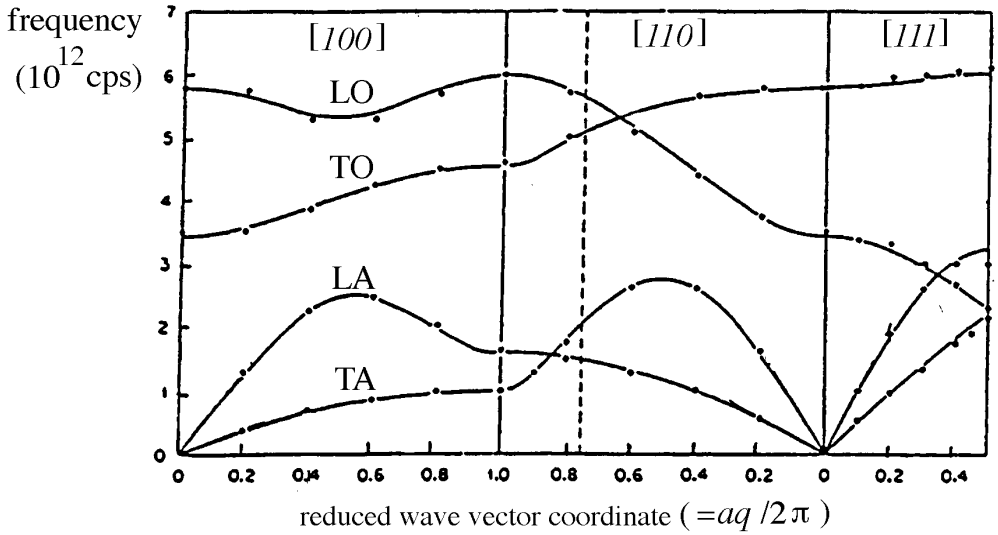

Figure F.4. Phonon dispersion curves of cubic AgCl.

We will perform our experiment by using the maximum value of k_i.

F5.

Work out the possible values of k_f and ϕ. (There are two solutions depending on whether ΔE, which is the phonon energy, is chosen to be positive or negative.)

F6.

It turns out that better resolution occurs for energy loss than for energy gain. Draw the configuration of $\mathbf{k}_i$ and $\mathbf{k}_f$ in Figure F3 for energy loss.

Another factor influencing the intensity which we observe in our experiment is the so-called Bose factor $n(E)$. *This gives the population of phonon states at any given energy and temperature:*

$$n(E) = \frac{1}{\exp\left(E/k_B T\right) - 1} \quad .$$

The intensity for neutron energy loss is proportional to $[1 + n(E)]$, *whereas for neutron energy gain it is proportional to* $n(E)$.

F7.

(i) Calculate the Bose factors for the energy gain and energy loss configurations in our example assuming that the sample is at a temperature of: (a) 300 *K*, (b) 0 *K*.

(ii) Given the intensity relationships above, which way would we do the experiment with the sample at (a) room temperature, (b) liquid-helium temperature ?

F8.

Is it possible to measure the *TA*[*001*] phonon around the *440* reciprocal-lattice point ?

To map out the dispersion curves in Figure F.4, we would do energy scans, say from 2 to 8 meV, at a series of **q** values between [*220*] and [*221*]. *A single peak would appear on each scan, giving the phonon energy for that reduced wave-vector.*

F9.

Suppose an experiment is performed to measure the phonon dispersion curves of potassium on a triple-axis spectrometer, when the energy of the beam scattered into the analyser is held fixed at *3.5* THz. For a measurement of the LA mode at **Q** = [2.5, 0, 0], what will be the energy of the incident beam for an experiment in which the neutron beam loses energy in the creation of a phonon. The phonon dispersion curves of potassium are given in Fig. F.9, and the lattice parameter of potassium is 5.23Å.

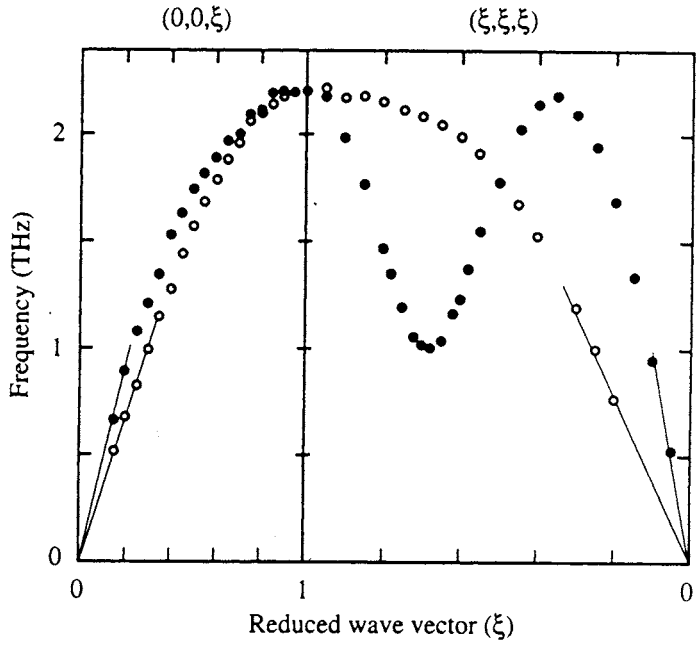

Fig. F.9 Acoustic mode dispersion curves for potassium (bcc) measured by inelastic neutron scattering. The right-hand plot shows the relevant portion of reciprocal space. (Data taken from Cowley *et al. Phys. Rev.* **15,** 487, 1966.)

G: Disordered Materials Diffraction

Exercises G

Introduction

Much of the content in this course concerns crystalline materials. In general terms these have a characteristic structural motif, the unit cell, that repeats itself more or less indefinitely throughout the material in a very well defined manner. For liquids and glasses there is an equivalent *local* structural motif, determined by the interaction forces between the atoms, but this does *not* repeat itself indefinitely. Instead the organisation of the material appears to become increasingly chaotic the further you move away from any given starting point. At sufficiently large distances there is no sign of order at all. Such a material is truly disordered, i.e. over a large enough distance range the positions of atoms become totally *uncorrelated* with each other.

The purpose of this tutorial is to explore the ramifications of these statements and how they affect the diffraction experiment on a liquid or other truly disordered material. Of course even crystals demonstrate disorder to a greater or lesser extent, but this disorder is occurs within the framework of a fundamentally ordered lattice. For a liquid or glass there is no lattice of unit cells arranged in a regular manner. Effectively there is only one unit cell, it is as big as the sample, and in the case of a liquid it is continually changing.

Note: Some of the examples are easier to complete if you have access to a spread sheet like Excel, but this is not essential.

For simplicity all the figures are arranged in a separate section at the end of each exercise.

Exercise G1: The interatomic potential, the pair distribution function, the coordination number, and the structure factor.

Typically atomic overlap is prevented by strong repulsive forces that come into play as soon as two atoms approach one another below some characteristic separation distance σ (which is usually expressed in units of Å = 10^{-10}m). At greater distances the atoms are normally attracted to one another by weak van der Waals (dispersion) forces, the magnitude of which is governed by an interaction parameter ε, which can be expressed in units of kJ per gm mole.

These facts can be conveniently (but only approximately) expressed by the model Lennard-Jones potential energy for two atoms separated by a distance *r*:

$$U(r) = 4\varepsilon\left(\left(\frac{\sigma}{r}\right)^{12} - \left(\frac{\sigma}{r}\right)^{6}\right) \qquad (1.1)$$

(Of course if charges, or electric or magnetic dipoles are present on the atoms, then additional terms will be required in this interatomic potential.)

G 1.1

a) With ε = 0.6kJ/mole and σ = 3.0Å, sketch this function approximately in the distance range 0 – 10Å.

b) What do the values of ε and σ signify?

c) Mark on your graph the repulsive core and dispersive regions.

G 1.2 According to the theory of liquids (see for example *Theory of Simple Liquids*, J P Hansen and I R McDonald, 2nd Edition, Academic Press, 1986), in the limit of very low density (e.g. like the density of the air in the atmosphere), the pair distribution function (pdf, also sometimes called the radial distribution function, rdf) between atom pairs is given by the exact expression:

$$g(r) = \exp\left[-\frac{U(r)}{k_B T}\right] \qquad (1.2),$$

where k_B is Boltzmann's constant. In the units of kJ per mole k_B = 0.008314 kJ/mole/K.

a) Sketch this function for the Lennard-Jones potential used in 1.1 a) at (say) T = 300K. $g(r)$ is the primary function which is being measured in a diffraction experiment.

b) From your sketch, describe briefly the main differences between $U(r)$ and $g(r)$.

c) What would happen to $g(r)$ for example if you increased ε by a factor of 2, or increased σ by 20%?

Note that in the limit of zero density *g(r)* does not go to zero.

G 1.3 Of course real materials occur with much higher densities than those of low density gases. This gives rise to an additional contribution to $g(r)$ from *three-body* and higher order correlations. In general these are difficult or impossible to calculate analytically without making several approximations, so that resort has to be made to *computer simulation* to estimate the effect of many body correlations.

Figure 1.1 shows a simulated $g(r)$ for our "Lennard-Jonesium" of **1.1**, at two densities, (a) $\rho = 0.02$ and (b) $\rho = 0.035$ atoms/Å^3 respectively.

a) Comparing these with your "zero density" sketch of $g(r)$ from **1.2**, describe the main effects of many-body correlations on $g(r)$. In particular:-

   i) How does the position of the first peak move with the change in density?

   ii) How do the positions of the second and subsequent peaks move with change in density?

   iii) Is the amount of peak movement what you expect based on the density change?

b) Why do you think many-body correlations have the effect they do?

G 1.4 Coordination numbers are defined as the integral of *g(r)* in three dimensions over a specified radius range:-

$$N(R_1, R_2) = 4\pi\rho \int_{R_1}^{R_2} r^2 g(r) dr \qquad (1.3)$$

The "running" coordination number at radius r is defined as $N(0, r)$, which is

sometimes written simply as $N(r)$. Figure 1.2 shows the running coordination numbers for the rdfs of Figure 1.

a) Using the grid provided estimate approximately the coordination number up to the first minimum in *g(r)* for each of the cases shown in Figure 1. This is what is frequently quoted as the "coordination number" of the atom at each density. Do these numbers scale with the density?

b) If instead we had used the same distance range for both densities would the coordination numbers scale with density?

G 1.5 The diffraction experiment does not measure *g*(*r*), but its *Fourier transform*, the structure factor, *H(Q)*, where

$$H(Q) = 4\pi\rho \int_0^\infty r^2 (g(r) - 1) \frac{\sin Qr}{Qr} dr \qquad (1.4)$$

where *Q*, the wavevector change in the diffraction experiment, is given by, $Q = \frac{4\pi \sin\theta}{\lambda}$, with 2θ the detector scattering angle, and λ the radiation wavelength.

The structure factors corresponding to the two densities of Lennard-Jonesium in **1.3** are shown in Figure 1.3.

a) Describe the effect of changing the density on the structure factor. How does this compare with effect of changing the density on the rdf?

b) What is the (approximate) relationship between the position of the first peak in *g(r)* and the first (primary) peak in *H(Q)*?

c) What would happen to the position of the first peak in *H(Q)* if we increased the value of σ?

d) Given that the radial distribution function remains finite at all densities, using (1.4) what is the structure factor of an infinitely dilute gas?

G 1.6 The inversion of (3) to *g(r)* is given by

$$g(r) = 1 + \frac{1}{2\pi^2 \rho} \int_0^\infty Q^2 H(Q) \frac{\sin Qr}{Qr} dQ \qquad (1.5)$$

Given that the measured *H(Q)* is likely to have a noise contribution, plus it will not be available for all *Q* values, list some of the difficulties that might be encountered in estimating *g(r)* from an experiment that measures *H(Q)*.

Figure G 1.2

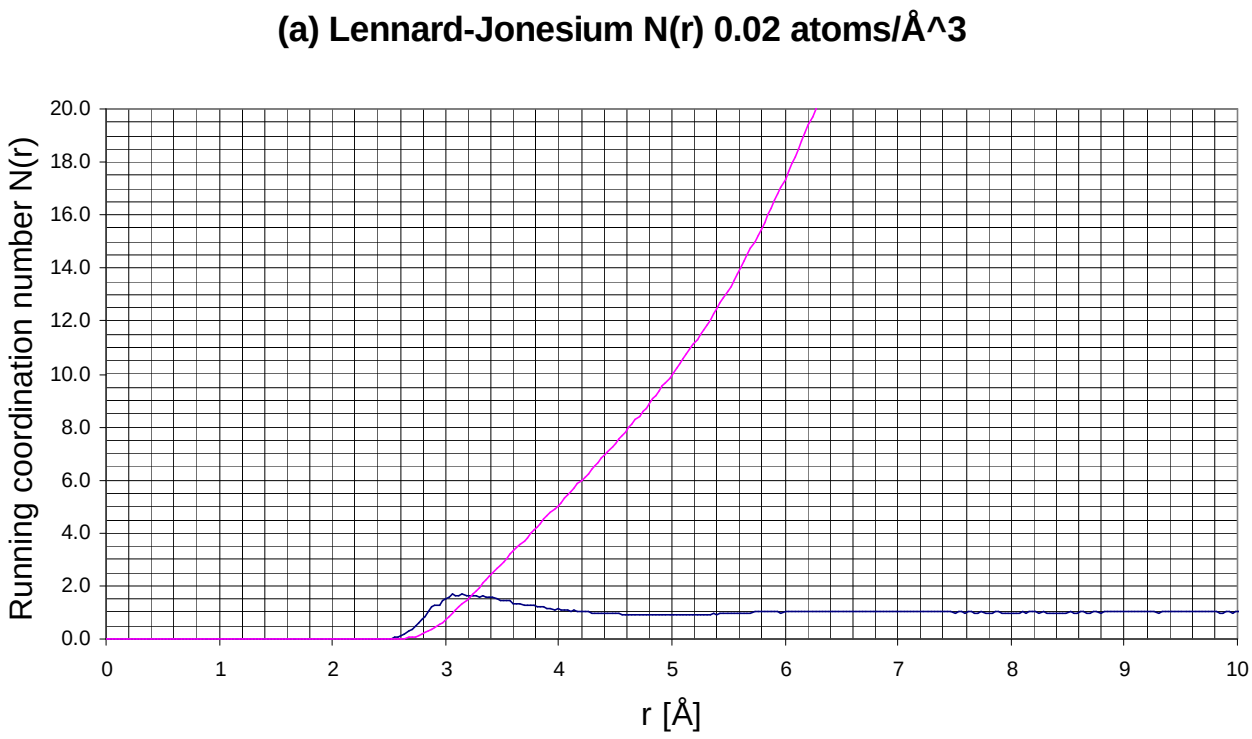
(a) Lennard-Jonesium N(r) 0.02 atoms/Å^3
Running coordination number N(r)
20.0
18.0
16.0
14.0
12.0
10.0
8.0
6.0
4.0
2.0
0.0
0
1
2
3
4
5
6
7
8
9
10
r [Å]

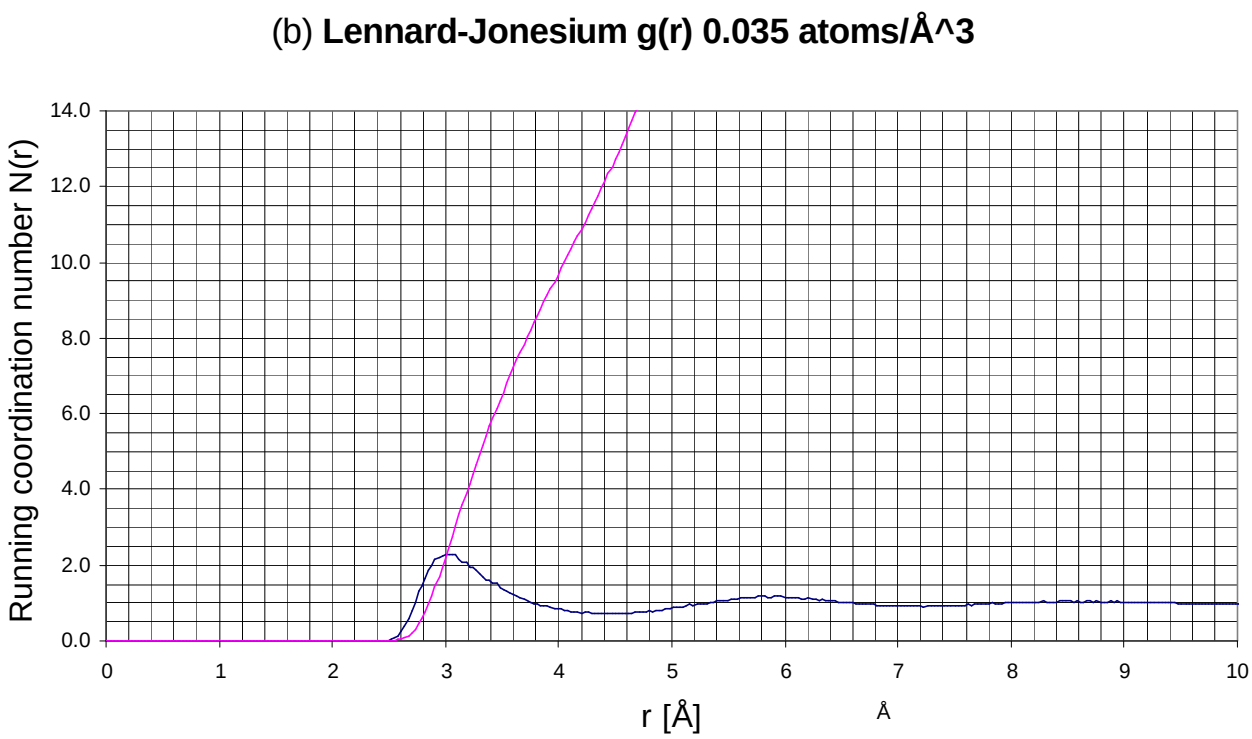
(b) Lennard-Jonesium g(r) 0.035 atoms/Å^3
Running coordination number N(r)
14.0
12.0
10.0
8.0
6.0
4.0
2.0
0.0
0
1
2
3
4
5
6
7
8
9
10
r [Å]
Å

Figure G 1.3

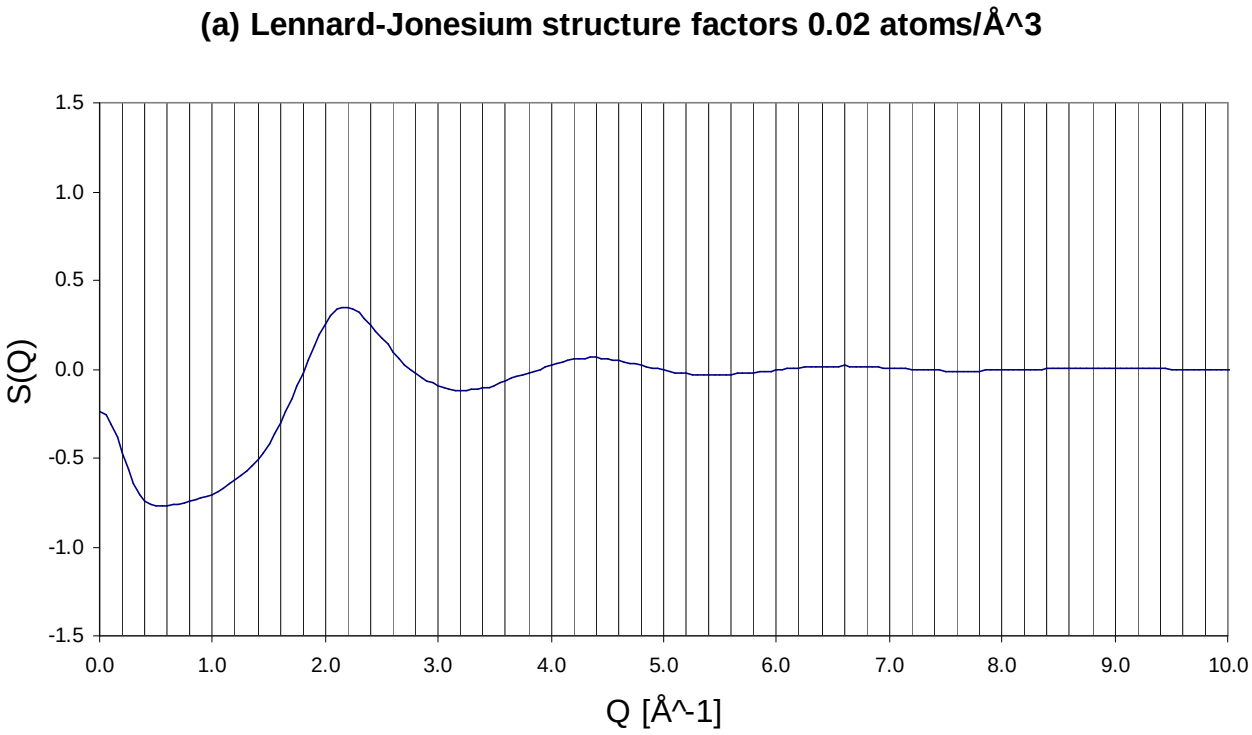
(a) Lennard-Jonesium structure factors 0.02 atoms/Å^3
S(Q)
1.5
1.0
0.5
0.0
-0.5
-1.0
-1.5
0.0
1.0
2.0
3.0
4.0
5.0
6.0
7.0
8.0
9.0
10.0
Q [Å^-1]

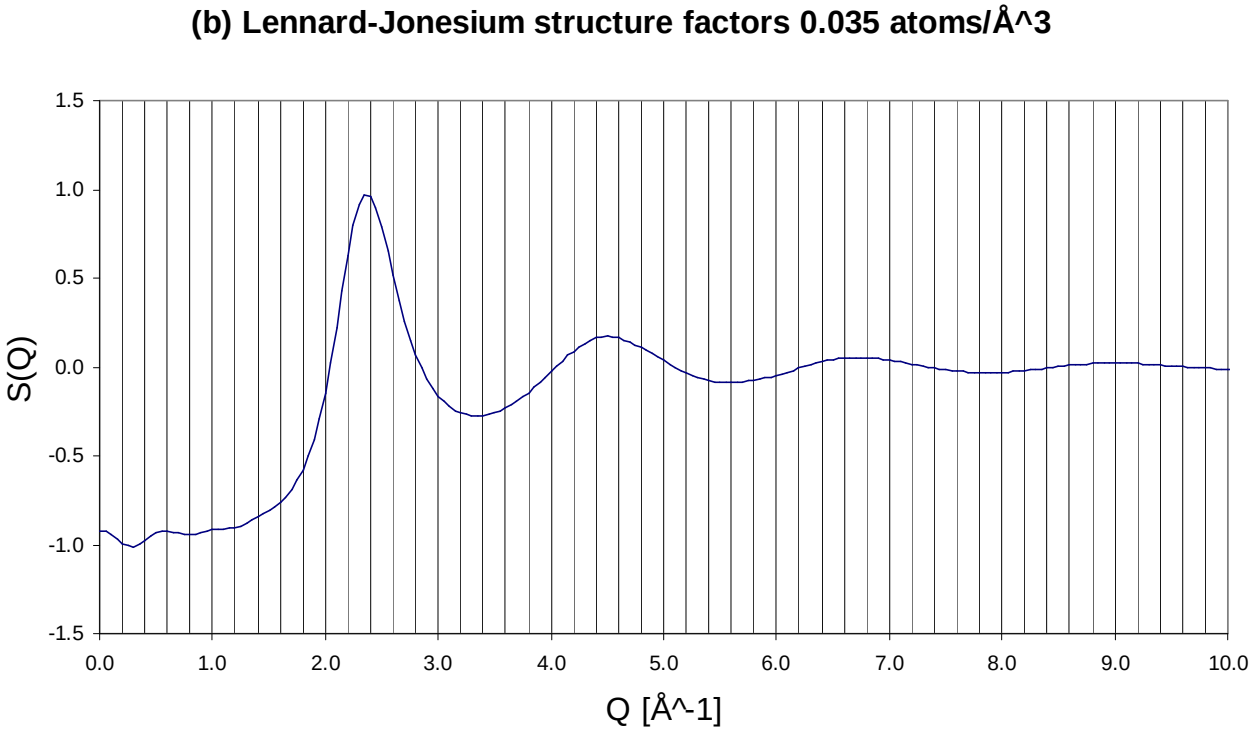
(b) Lennard-Jonesium structure factors 0.035 atoms/Å^3
S(Q)
1.5
1.0
0.5
0.0
-0.5
-1.0
-1.5
0.0
1.0
2.0
3.0
4.0
5.0
6.0
7.0
8.0
9.0
10.0
Q [Å^-1]

Exercise G 2: Two component systems: use of isotope substitution and the case of molten $ZnCl_2$.

The diffraction pattern from a system containing 2 atomic components can be written as

$$F(Q) = c_1^2 \langle b_1 \rangle^2 H_{11}(Q) + 2c_1 c_2 \langle b_1 \rangle \langle b_2 \rangle H_{12}(Q) + c_2^2 \langle b_2 \rangle^2 H_{22}(Q) \qquad (2.1),$$

where c_α is the atomic fraction and b_α is the neutron scattering length of component α, $H_{\alpha\beta}(Q)$ is the partial structure factor (psf), analogous to (1.4) above, for the pair of atoms α,β, defined by:

$$H_{\alpha\beta}(Q) = 4\pi\rho \int_0^\infty r^2 \left(g_{\alpha\beta}(r) - 1\right) \frac{\sin Qr}{Qr} dr \qquad (2.2),$$

and $g_{\alpha\beta}(r)$ is the site-site radial distribution function of β atoms about α. Note that formally with the definitions being used here $g_{\alpha\beta}(r) \equiv g_{\beta\alpha}(r)$. The brackets around the scattering lengths indicate that the scattering lengths have to be averaged over the spin and isotope states of each atomic component. The coordination number of β atoms about atom α can be defined in an analogous manner to (1.3):-

$$N_{\alpha\beta}(R_1, R_2) = 4\pi\rho c_\beta \int_{R_1}^{R_2} r^2 g_{\alpha\beta}(r) dr \qquad (2.3)$$

A general rule is that if there are N distinct atomic components in a system, then there are $N(N+1)/2$ site-site radial distribution functions and partial structure factors to be determined. By "distinct atomic components" we do not necessarily mean atom types. For example a methyl hydrogen atom on an alcohol molecule is distinct from the point of view of the structure to a hydroxyl hydrogen atom, even though they are the same atom type.

G 2.1 A classic example of the application of the isotope substitution method to a two-component liquid is the molten $ZnCl_2$ experiment of Biggin and Enderby (*J. Phys. C: Solid State Phys.*, **14**, 3129-3136 (1981).

a) What are the atomic fractions of Zn and Cl in $ZnCl_2$ salt?

b) Hence, based on equation (2.1), write down a formula for the diffraction pattern of ZnCl2 in terms of the Zn-Zn, Zn-Cl and Cl-Cl partial structure factors.

c) Given that two isotopes of chlorine are available, ^{35}Cl and ^{37}Cl, with markedly different scattering lengths (11.65fm and 3.08fm respectively)

briefly explain how you might extract the three partial structure factors for $ZnCl_2$ experimentally.

d) Are there any other experimental techniques that could be used to do this?

G 2.2 Figure 2.1 shows the actual diffraction data of Biggin and Enderby, while Table I below lists the neutron weights outside each partial structure factor for each of the Biggin and Enderby samples:

Table I

Sample	**At%^{35}Cl [%]**	**At.%^{37}Cl [%]**	**Individual psf weighting factors [barns/sr/atom]†**		
			Zn-Zn	**Zn-Cl**	**Cl-Cl**
Zn35Cl2	99.3	0.7	0.0358	0.2929	0.5982
ZnMixCl2	67.7	32.3	0.0358	0.2253	0.3541
Zn37Cl2	2.7	97.3	0.0358	0.0837	0.0489

†1 barn = $10^{-28}m^2$.

a) On the basis of the numbers in this table describe any problems that might arise in attempting to invert the diffraction data to partial structure factors. Look also at the diffraction data themselves, Figure 2.1.

b) Given those reservations, what might happen when we try to convert the extracted partial structure factors to radial distribution functions using the Fourier transform equation (1.5)?

c) Describe another method that might be used to separate out the site-site radial distribution functions from the measured diffraction data.

G 2.3 Figure 2.2 shows a computer simulation of the radial distribution functions of molten zinc chloride, $ZnCl_2$, as derived from the Biggin and Enderby diffraction data.

a) Using the grid, or other method, estimate approximately the coordination number of Cl around Zn. The atomic number density for this material is 0.0336 atoms/Å^3.

b) Given this number, and the position of the Zn-Zn and Cl-Cl first peaks, what can you say about the local structure in molten $ZnCl_2$?

c) For the region beyond the first peaks, what do you notice about the three site-site rdfs for molten $ZnCl_2$? Use this to speculate on what might be happening to the ordering of the Zn and Cl atoms.

d) Speculate on why the second peak in the ZnCl distribution might be split. (This is a tough question!)

Figure G 2.1 Diffraction data (points) for molten zinc chloride using different chlorine isotope mixtures. The line is a modern fit to these data using an EPSR (empirical potential structure refinement) computer simulation.

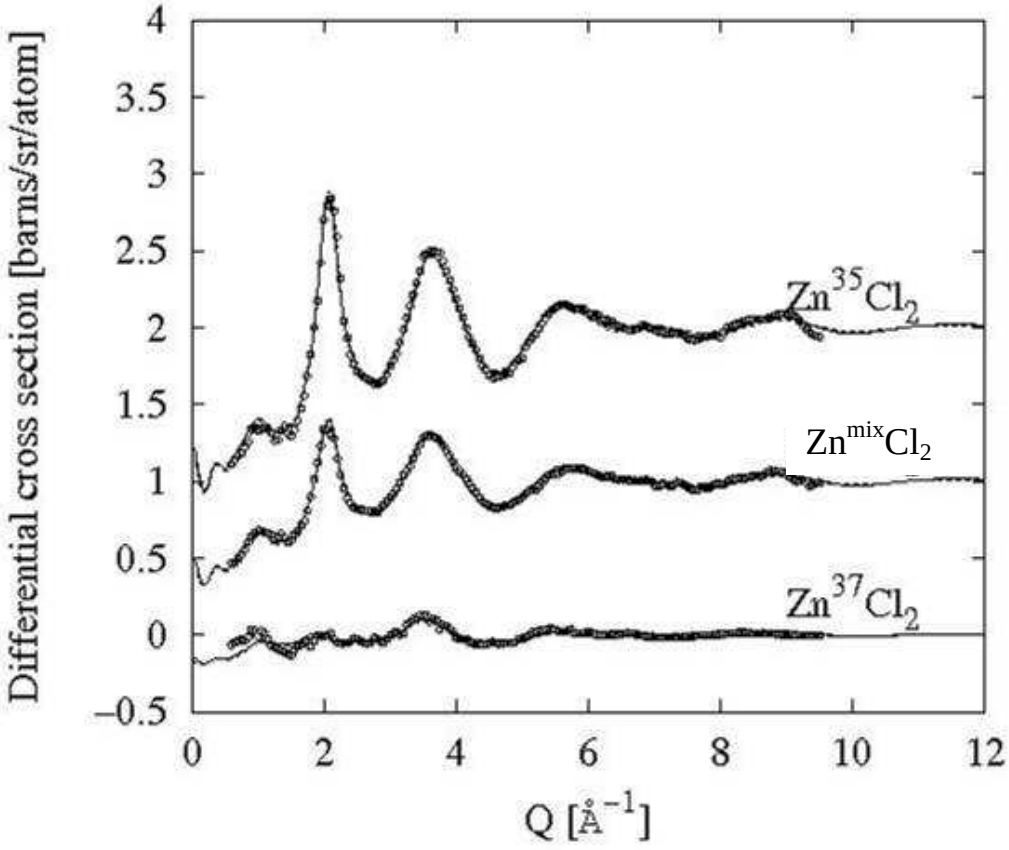

Figure G 2.2 Radial distribution functions for molten zinc chloride.

Zn-Zn

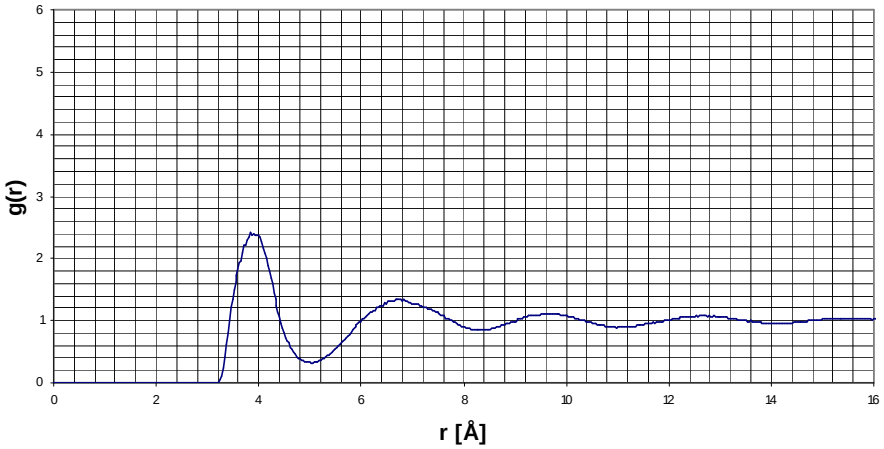

Zn-Cl

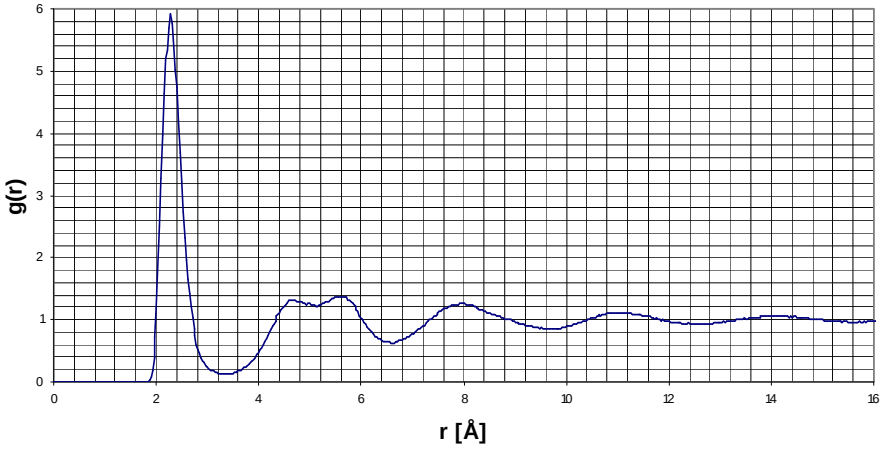

Cl-Cl

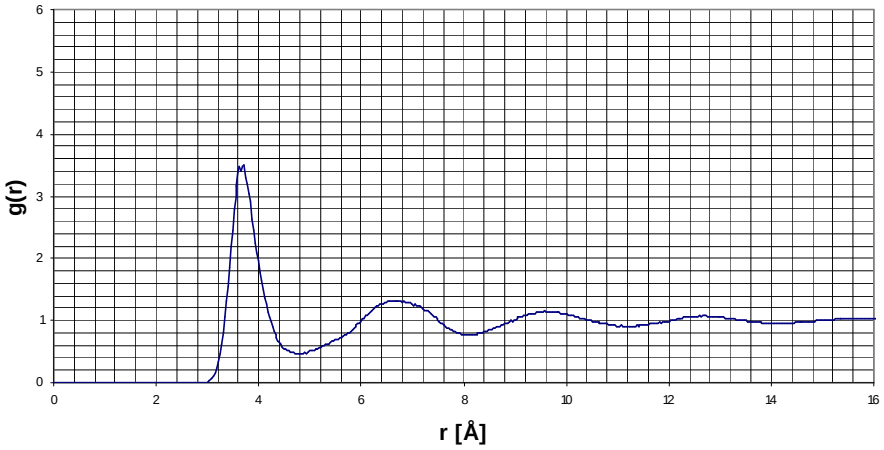

Exercise G 3. Molecular systems and orientational correlations.

Molecular systems present a particular challenge to the diffraction experiment. Not only can a molecule have a position, but in addition it has an orientation, which in general is expressed in terms of 3 Euler angles, $\boldsymbol{\omega}_M = (\varphi_M, \theta_M, \chi_M)$. The Euler angles can be defined in a variety of ways, but a common convention used throughout the work at ISIS is a follows: first the molecule is rotated about its initial *z*-axis by an amount φ_M. Then it is rotated about its new *y* axis by an amount θ_M. Finally it is rotated about its new *z* axis by an amount χ_M. All rotations are performed using the right hand screw rule.

The previous radial distribution function is now replaced by the *pair correlation function*, $g(\mathbf{r}_{12}, \boldsymbol{\omega}_1, \boldsymbol{\omega}_2)$ of molecule 2 about molecule 1, where $\mathbf{r}_{12}$ is the vector from 1 to 2 (in the laboratory reference frame). This pair correlation function is in general therefore a function of 9 scalar dimensons. If however we make the laboratory reference frame coincident with the coordinate axes of molecule 1 at the origin, (in other words set $\boldsymbol{\omega}_1 = 0$), then $\boldsymbol{\omega}_2$ is simply the orientation of molecule 2 relative to molecule 1, (we'll call this $\boldsymbol{\omega}_M$) and our 9-dimensional problem has become a 6-dimensional problem. See Figure 3.1.

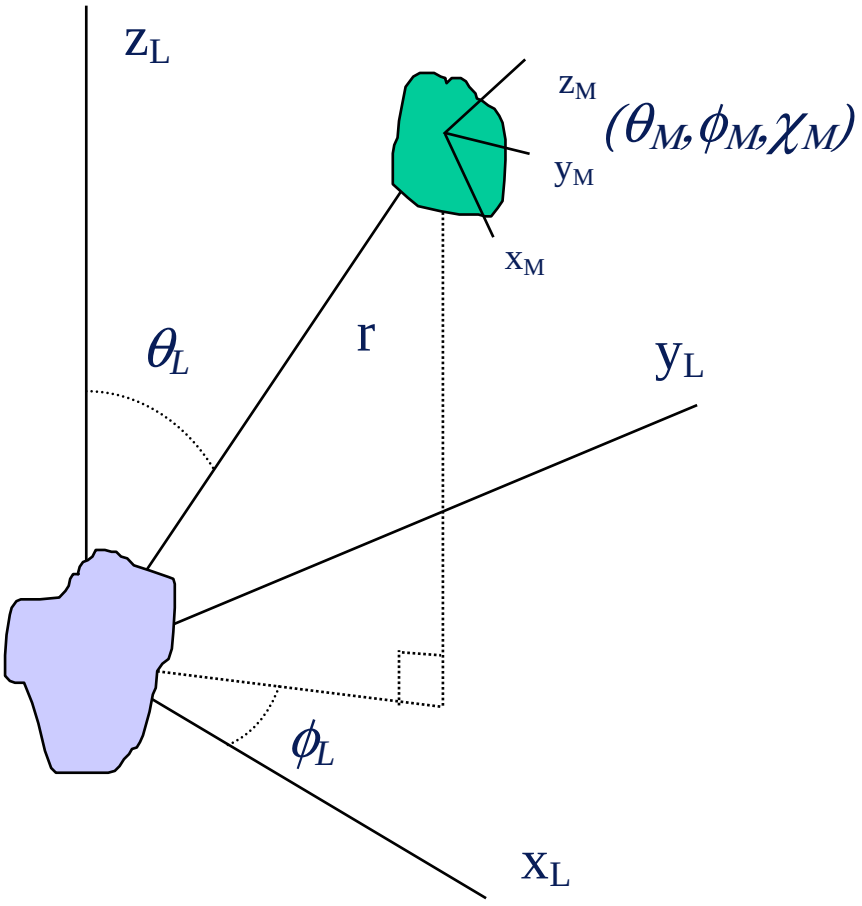

Figure G 3.1 Coordinate axes for the orientational pair correlation function.

This still is too many dimensions to visualise easily however. Therefore a simpler function is often discussed, prior to investigating the details of the relative orientations. This is called the *spatial density function* (SDF) and is obtained by averaging $g(\mathbf{r}_{12},0,\boldsymbol{\omega}_2)$ over the orientations of molecule 2, leaving a function of only 3 dimensions (r_{12}, θ_L, φ_L), where (θ_L, φ_L) is the direction away from molecule 1. This can be plotted using a surface contour. Hence the SDF represents the distribution of neighbouring molecules around one at the origin after averaging over the orientations of those neighbours. It is sometimes written simply as

$$g(r_{12},\theta_L,\varphi_L)=\langle g(\mathbf{r}_{12},0,\boldsymbol{\omega}_2)\rangle_{\boldsymbol{\omega}_2} \qquad (3.1).$$

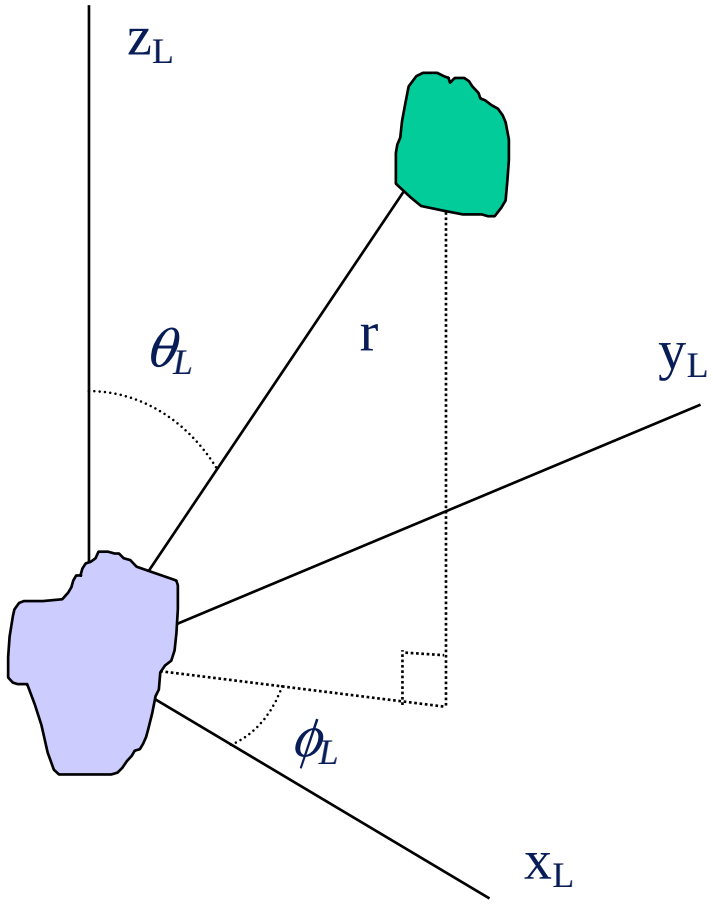

Figure G 3.2 Coordinate axes of the spatial density function

Unfortunately it is not possible to measure either the spatial density function or the full orientational pair correlation function with neutrons (or any other technique for that matter). Hopefully this exercise will demonstrate the powerful role neutrons can play in identifying the spatial density function in particular instances.

G 3.1 Given that the diffraction experiment probes only atom positions.

a) Describe the fundamental limitations on attempting to extract the full orientational pair correlation function from a set of diffraction data;

b) Describe how we might nonetheless approximately extract the spatial density function and orientational correlation functions from a set of diffraction data.

G 3.2 The choice of internal axes for a molecule depends on its symmetry. Describe or sketch a suitable set of axes for the following molecules: H_2O, NH3, CH4, benzene (C_6H_6), methanol (CH_3OH), and ethanol (CH_3CH_2OH).

G 3.3 Water, H_2O, and its solutions and mixtures are probably some of the most widely studied fluids with neutrons.

a) Explain why water can be studied so usefully with neutrons.

b) Given that the OH distance in the water molecule in the liquid is ~0.98Å and the HH distance is ~1.55 Å, sketch a water molecule.

c) Take as given that the oxygen atom on water is negatively charged, and the hydrogen atoms are positively charged, and assume that when a hydrogen bond forms the OH bond on one molecule points directly towards the oxygen on another. Draw a sketch of the likely arrangement of a few (4) water molecules hydrogen bonded to a central water molecule. Mark on the sketch and write down a few of the critical distances that are likely to occur in this cluster. Note that the O-O nearest neighbour distance is ~2.8Å, while the O-H *inter*molecular distance along a hydrogen bond is ~1.8Å. You should have at least 2 distances for each of O-O, O-H and H-H pairs.

d) Figure 3.1 shows the estimated O-O, O-H and H-H radial distribution functions for water, as derived by computer simulation of the diffraction data from mixtures of heavy and light water. How do the peaks in these functions compare with your distances in c)? What feature of the real rdfs is lacking in simple models such as we have generated in c)?

e) Using your sketches and the data of Figure 3.1, imagine or sketch a water molecule at the origin, with its oxygen atom at the origin and hydrogen atoms in the (positive) *z-y* plane. Try to map out in which directions (θ_L, φ_L) you would expect to see neighbouring first shell water molecules. Compare your predictions with the actual results for the simulations of Figure 3.1 as shown in Figure 3.2a, which shows the SDF for water in the distance range 2 – 3.25Å.

f) Figure 3.2b shows the same SDF but in the distance range 3.25Å – 4.5Å. This is the region up to the second maximum in $g_{OO}(r)$. Compared to 3.2a do you notice anything about the distribution of density in this second figure?

g) Finally, in the lobes marked I and II in figure 3.2a, write down or sketch the most likely orientations of water molecules in these lobes. Where do the uncertainties in these orientations arise from?

Figure G 3.1 Radial distribution functions for water. OW means water oxygen. HW1 means water hydrogen.

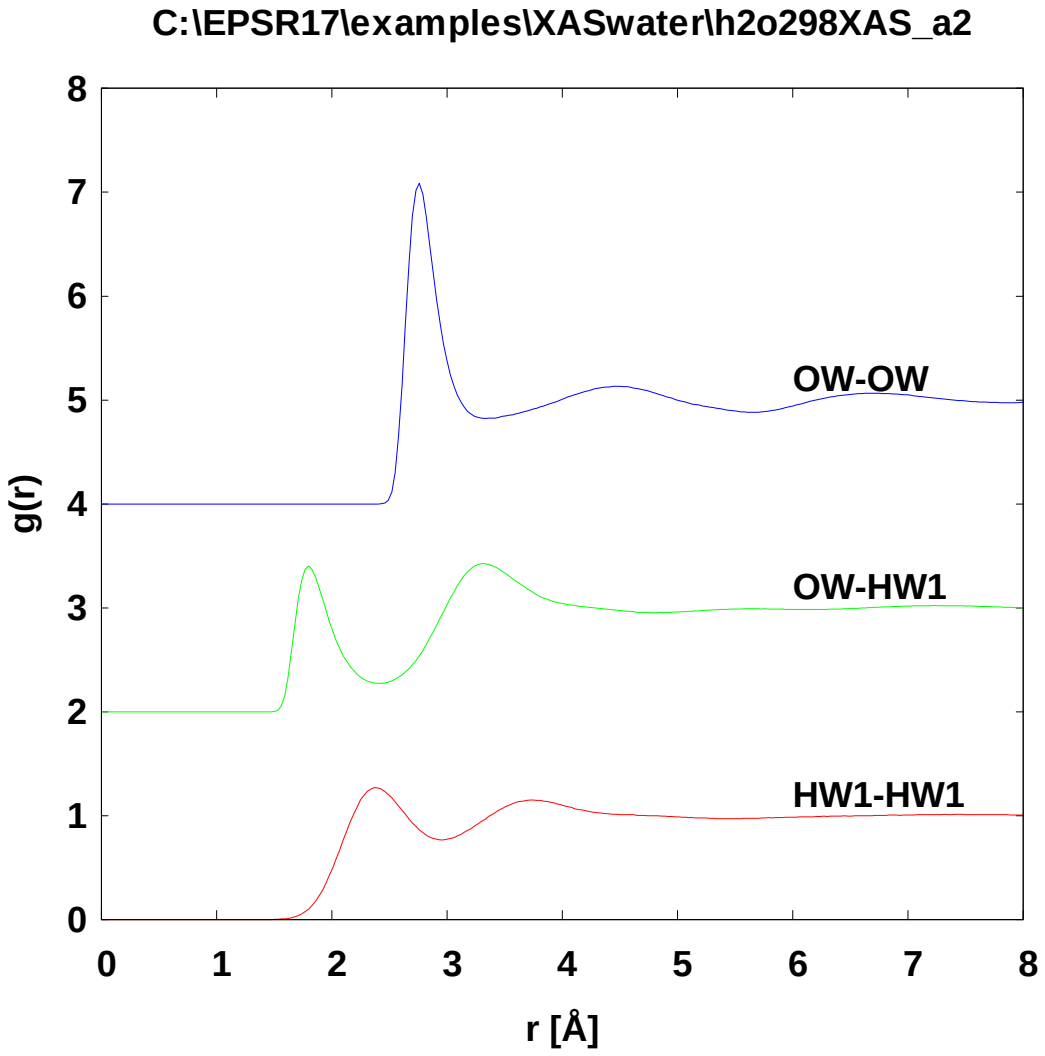

Figure G 3.2a Spatial density function of water about water for the distance range 2 – 3.25Å.

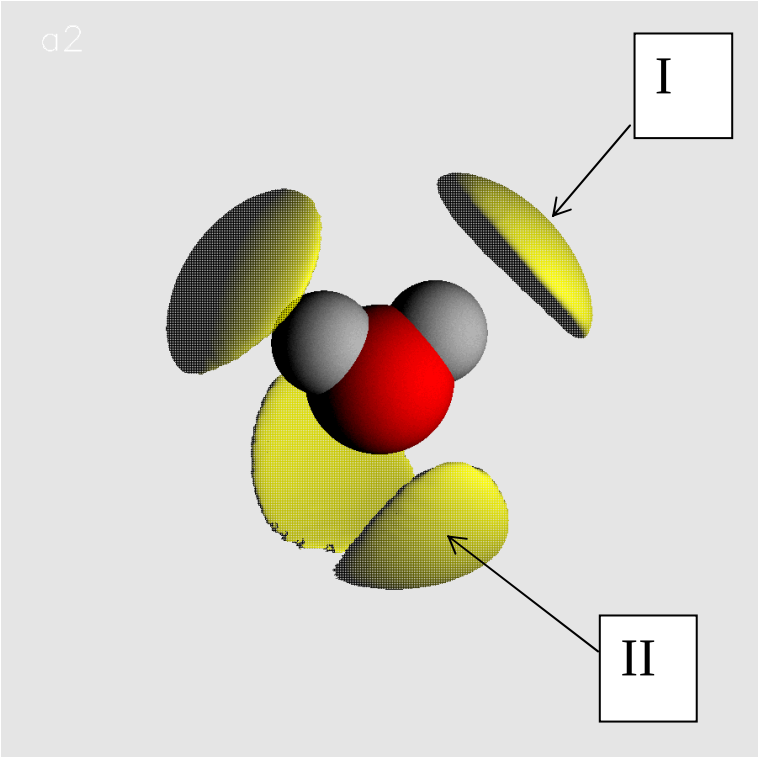

Figure G 3.2b Spatial density function of water about water in the distance range 3.25Å – 4.5Å.

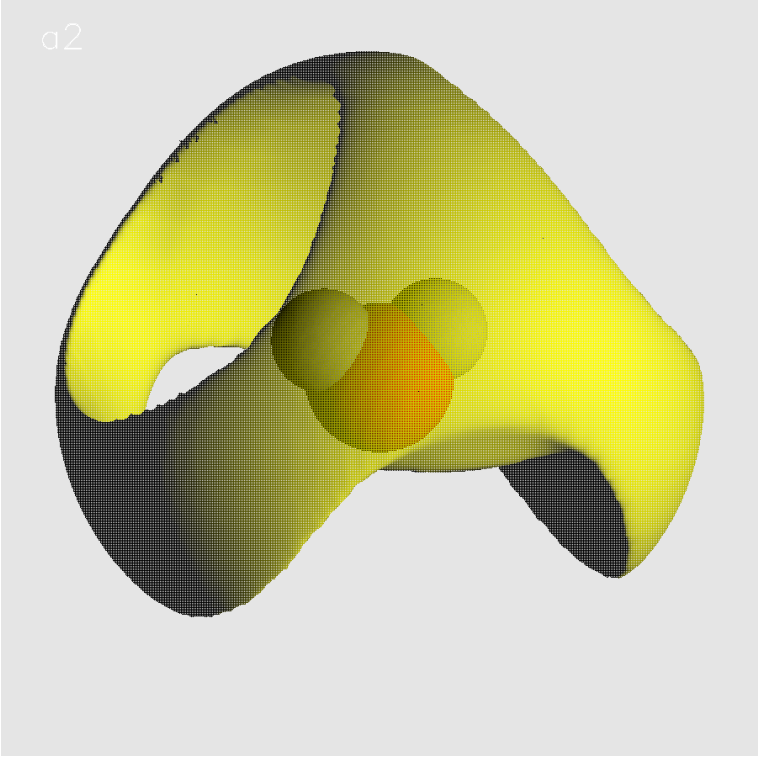

H: Polarized Neutrons

Exercises H

H1. a) In the instrument in fig. 1, what is the beam polarization if the there are 51402 counts/second with the flipper off and 1903 counts per second with the flipper on? Provide also a calculation of the error bar in the beam polarization value.

b) What would be the main sources of systematic error in this measurement?

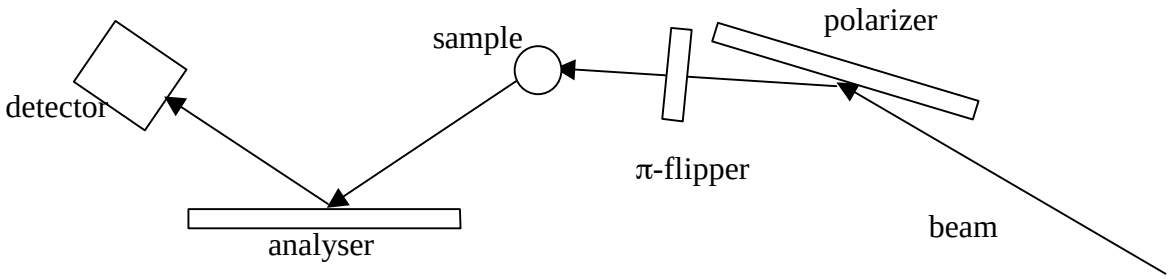

Figure H1

H2. a) Fig. 2 shows a configuration for a Dabbs-foil flipper, designed for neutrons of wavelength 2Å. By checking the rate of the field rotation, state whether you believe that this is a good design for a π-flipper.
b) Suggest ways in which the design may be improved.

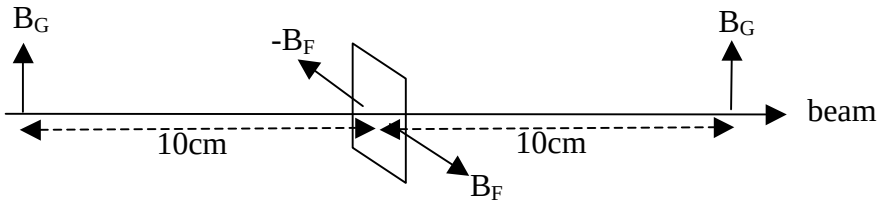

Guide field- B_G = Flipper field- B_F = 3mT

Figure H2

H3. a) Assuming that a polarizing filter has an absorption cross-section consisting of a spin-dependent part and a spin-independent part of the form

$$\sigma_{\pm} = \sigma_0 \pm \sigma_P$$

show that the neutron polarization and transmission through the filter are given by

$$P = -\tanh(\sigma_p N t) \text{ and } T = \exp(-\sigma_o N t)\cosh(\sigma_p N t).$$

Hint: the number of neutrons transmitted through the filter will be proportional to exp(-Nσt) where N is the number density of scatterers in the filter, and t is the thickness

b) Given that the nuclear spin of a ^{3}He nucleus is I = ½, show that the polarization of the ^{3}He nuclei is given by:

$$P_{He} = -\frac{\sigma_p}{\sigma_0},$$

and hence find expressions for the polarization and transmission of a ^{3}He spin-filter. Hint: equate the expressions $\sigma_{\pm} = \sigma_a(E)(1 \pm \rho P_N)$ and $\sigma_{\pm} = \sigma_0 \pm \sigma_P$.

H4. Show that the polarizing efficiency of a crystal monochromator is given by

$$P_f = \frac{2F_N(\mathbf{Q})F_M(\mathbf{Q})}{\left[F_N^2(\mathbf{Q}) + F_M^2(\mathbf{Q})\right]},$$

where the symbols have their usual meanings.

H5. Why is it not necessary to analyse the neutron spin when scattering from a ferromagnet saturated in a direction perpendicular to Q?

H6. a) Verify the following relations (so-called Pauli spin relations):

$$\sigma_x|\uparrow\rangle = |\downarrow\rangle, \quad \sigma_x|\downarrow\rangle = |\uparrow\rangle$$
$$\sigma_y|\uparrow\rangle = i|\downarrow\rangle, \quad \sigma_y|\downarrow\rangle = -i|\uparrow\rangle$$
$$\sigma_z|\uparrow\rangle = |\uparrow\rangle, \quad \sigma_z|\downarrow\rangle = -|\downarrow\rangle$$

where σ_x, σ_y and σ_z are the Pauli spin matrices and the spin-up and spin down neutron eigenstates are given by $|\uparrow\rangle = \begin{pmatrix}1\\0\end{pmatrix}$ and $|\downarrow\rangle = \begin{pmatrix}0\\1\end{pmatrix}$

b) Hence show that the spin flip scattering is sensitive only to those components of the magnetisation $M_\perp$ perpendicular to the neutron polarization vector (along z).

H7. Using the Moon, Riste and Koehler expressions, together with the definition of the Fourier component of the magnetisation perpendicular to **Q**, $M_{\perp}$, show that the magnetic scattering is entirely spin-flip if the neutron polarization is parallel to **Q**.

H8. What is the advantage of the X-Y-Z difference method of magnetic scattering separation over the method of measuring with the neutron polarization **P** || **Q**?

H9. What is the advantage of using neutron spin-echo in order to investigate para-magnetic quasi-elastic scattering?
Hint: Magnetic scattering from a paramagnet will be entirely spin-flip when the polarization is perpendicular to **Q** and entirely non-spin-flip when parallel to κ. – And the plane of precession of the neutrons is parallel to **Q**.

Values of Physical Constants :

	SI units
speed of light c	2.998×10^{8} m s^{-1}
charge of electron e	1.602x10^{-19} coulombs
Boltzmann's constant k_B	1.38×10^{-23} J K^{-1}
Planck's constant h	6.626×10^{-34} J s
Avogadro's number N_A	6.02×10^{23} mol^{-1}
mass of electron m_e	9.109x10^{-31} kg
mass of proton m_p	1.673x10^{-27} kg
Bohr magneton μ_B $\left(= e\hbar / 2m_e\right)$	9.274x10^{-24} J/tesla
nuclear magneton μ_N $\left(= e\hbar / 2m_p\right)$	5.051x10^{-27} J/tesla

Properties of the neutron:

mass m_n	1.675x10^{-27} kg
charge	0
spin	1/2
magnetic moment	-1.1913 μ_N

Relations between Units

1 eV ≡ 1.602x10^{-19} J ≡ 1.602x10^{-12} erg

≡ 2.418x10^{14} Hz ≡ 8.065x10^{3} cm^{-1} ≡ 11,600 K

1Å ≈ 82meV ≈ 660cm^{-1};

1meV ≈ 1.5THz ≈ 12K.